LAWRENCE
LIVERMORE
NATIONAL
LABORATORY

LLNL-CONF-656093

Space qualification of an antireflection coating on the surface of a ruled grating prism - Increasing the throughput of the Single Object Slitless Spectroscopy mode of NIRISS onboard JWST

L. Albert, R. Doyon, P. J. Kuzmenko, S. L. Little, G. S. Enzor, M. Maszkiewicz

June 23, 2014

Advances in Optical and Mechanical Technologies for Telescopes and Instrumentation
Montreal, Canada
June 22, 2014 through June 27, 2014

Disclaimer

Space qualification of an antireflection coating on the surface of a ruled grating prism - Increasing the throughput of the Single Object Slitless Spectroscopy mode of NIRISS onboard JWST

Loïc Albert[a], René Doyon[a], Paul J. Kuzmenko[b], Steve L. Little[b], Greg S. Enzor[c], Michael Maszkiewicz[d]

[a] Université de Montréal, Pavillon Roger-Gaudry, C. P. 6128, succ. Centre-ville, Montréal, H3C 3J7, Canada;
[b] Lawrence Livermore National Laboratory, L-183 PO Box 808, Livermore, CA 94551;
[c] Thin Film Lab Inc., 112 Sawkill Road, Milford, PA, 18337, USA;
[d] Canadian Space Agency, 6767 route de l'Aéroport, Saint-Hubert, J3Y 8Y9, Canada;

ABSTRACT

Grating prisms (grism) designed for near-infrared spectroscopy typically make use of high-refractive index materials such as zinc selenide (ZnSe), at the expense of large Fresnel losses ($\sim$ 18%). Part of the loss can be recovered by using anti-reflection (AR) coatings. The technique is however considered risky when applied on the ruled surface of a grating, especially for a space application at cryogenic temperature. Such a grism, made of ZnSe and machined at Lawrence Livermore National Laboratory (LLNL) is mounted in the Near-Infrared Slitless Spectrograph (NIRISS) onboard the James Webb Space Telescope (JWST). Its Single Object Slitless Spectrograph (SOSS) observing mode uses the ZnSe grism and a cross-dispersing prism to produce R=700 spectra in orders 1 and 2 to cover the 0.6 to 2.5 microns spectral domain. The ZnSe grism is blazed at 1.23 microns, has a density of 54 lines/mm and its triangular grooves have a depth of 700 nm, a base of 18 microns, with facets angled at 1.9 degrees. Here, an AR coating produced by Thin Film Lab (TFL) and deposited on the ruled surface of a ZnSe grism sample was space qualified. Atomic force microscopy (AFM) showed no groove profile change pre/post coating despite the large relative thickness of the AR coating to that of the groove depth ($\sim$ 35%). Also, the wavefront error map remained almost unchanged at lambda/8 (peak-to-valley at 632 nm) and survived unscathed through a series of three cryogenic cycles to 20 K. Finally, the transmission gain across our operating spectral range was almost as high as that for a unruled surface covered with the same AR coating (10-15%).

Keywords: Space Application, Grism, AR Coating, Spectroscopy, ZnSe, Near Infrared, Qualification, NIRISS, JWST

1. INTRODUCTION

The James Webb Space Telescope (JWST), scheduled for launch in 2018, incorporates four science instruments. The Near Infrared Imager and Slitless Spectrograph (NIRISS) is the Canadian built instrument on the back plane of the Fine Guidance Sensor (FGS) ([1]). NIRISS has imaging, aperture-masking interferometry (ref) and wide-field slitless spectroscopy (ref) capabilities, all in the near-infrared (1-5 microns). It also features the Single-Object Slitless Spectroscopy (SOSS) observing mode which was specifically designed and optimized for transit spectroscopy to study exoplanet atmospheres. The SOSS mode makes use of the GR700XD optics element, a crossed-dispersing device built of a ZnS prism and a ZnSe transmission *grism*. The first surface of this device is a weak cylindrical lens to project defocussed traces in orders 1 and 2, ensuring a simultaneous spectral coverage between 0.6 and 2.8 microns at a resolving power of about 700. The trace width is about 20 pixels in the spatial direction and Nyquist-sample limited along the spectral direction, with the objective to minimize flat fielding uncertainties and to allow brighter targets to be observed without saturating.

Further author information: (Send correspondence to L.A.)
L.A.: E-mail: albert@astro.umontreal.ca, Telephone: 1 514 343 6111 x3698

The key component of the GR700XD device is the zinc selenide (ZnSe) grism. A high refractive index material was required for the grism to ensure maximal spectral resolving power. Also, the refractive index dispersion of the prism and grism needed to be correctly matched to produce maximum order separation between order 1 and order 2, the two orders of interest. A team at the Lawrence Livermore National Laboratory (LLNL) successfully manufactured two such ZnSe grisms to specifications. They used the Precision Engineering Research Lathe (PERL) to diamond machine triangular grooves across the raw prisms surface ([2]).

An anti-reflection (AR) coating was certainly going to be deposited on the flat entrance surface of the grism to improve the instrument throughput. However, depositing an AR coating on the ruled exit surface was a large risk, especially for a space mission. The Fresnel loss per surface is of about 18% for ZnSe so AR coating the two surfaces of the grism promised to significantly improve the instrument throughput. However, the AR coating thickness was a significant fraction ($\sim 35\%$) of the groove depth. How would the groove shape be preserved and would the coating resist cycling to cryogenic temperatures? Would the wavefront be altered by coating-induced mechanical stress? This paper describes the steps taken to qualify the process of applying an AR coating on the ruled surface of our ZnSe grism. AR coating a ZnSe grating was successfully done in the past for the ground-based LMIRcam instrument ([3,4]). Also, 6 silicon grisms with their ruled-side AR-coated were successfully produced for NIRCam and are used for fringe sensing in aligning the segments of the JWST mirror ([5]).

2. QUALIFICATION OVERVIEW

In order to lift the risks associated with AR coating the ruled-side of the grism, a single representative ZnSe ruling sample went through various qualification steps. The following measurements were performed before and after an AR coating was applied to the sample: 1) Transmission and blaze function of the sample to quantify the AR efficiency; 2) Atomic Force Microscopy (AFM) to measure the profile of the grooves; 3) cryogenic cycles followed by microscope inspection to verify the coating's adherence; 4) Zygo interferometer measurements to monitor the wavefront error. After the first series of measurements, the ruling sample was AR coated by Thin Film Lab (Pennsylvania,USA) using electron beam evaporation, then the tests were repeated to monitor changes. Moreover, a separate AR coating sample was bombarded with protons to retire the risk associated with exposure to radiations.

2.1 The Ruling Sample

The ruling sample was produced by LLNL prior to manufacturing our two flight grisms. It consists in a ZnSe 1-inch flat of 5.6 mm in thickness and 25.4 mm in diameter. It was polished by BMV Optical (Ontario, Canada) to the same surface smoothness as the LLNL flight grisms. LLNL used the sample to test their PERL settings and in the process ruled 3 main areas of the sample (see Figure 1). The ruling pitch and groove angle is the same as for the flight grisms (at least for the largest ruled area that's 11.5 mm wide).

2.2 The AR Coating

After a first round of characterization at Université de Montréal (UdeM), the sample was shipped to Thin Film Lab to have an anti-reflection coating (BBAR@600-2500nm) applied on the entire surface of the ruled side. No special cleaning procedure was used prior to AR coating except dry air blowing for dust at TFL. The AR coating was applied and was followed by a 24-hour humidity test at TFL. The sample was shipped back to UdeM to go through a second round of measurements (same as pre-coating plus cryogenic life tests).

The process used for coating was electron beam evaporation. The coating was evaporated at high temperature in a vacuum chamber using an electron beam gun. Molecules travel upward at high speed in a straight line. The parts were put in the center of the planetary rotation so the angle of incidence of the vapor stream was minimized. The vapor stream angle was 15 degrees perpendicular to the coated surface but the rotation of the part produced on average a perpendicular stream. The physical thickness of the coating is 280 nm, which represents 35% of the groove depth of our grisms.

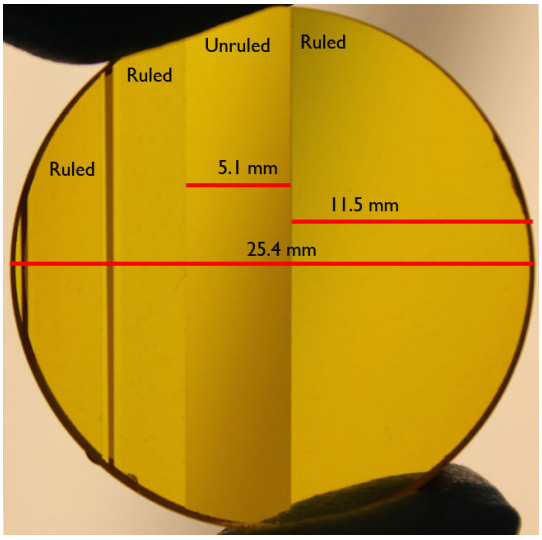

Figure 1. Ruled sample used to qualify the process of AR coating the ruled surface of our flight grisms. It is a 1-inch flat ZnSe sample on which a few sections are ruled. This ruled sample was monitored pre/post AR coating through 1) transmission tests, 2) groove profile measurements (AFM), 3) wavefront error maps and 4) cryo cycles.

3. UNRULED AREA TRANSMISSION BEFORE / AFTER COATING

The ZnSe transmission was measured prior and after being AR coated (Figure 2a). The largest unruled area (see Figure 1) was illuminated with the beam of the scanning spectrometer, a Lambda 950 spectrometer manufactured by Perkin Elmer. The spectrometer is mounted on an optical bench but not in a clean room. The spectrometer lacks an infrared integrating sphere which produces very noisy transmission measurements longward of 2500 nm. Scans were generally obtained at steps of 10 nm between 500 and 3300 nm with integration times of less than one second. Before gathering data, a dark and 100% transmission calibrations would be run and used to produce the final transmission curves. Also, the reflectivity of the AR coating was measured on a witness sample by TFL (Figure 2b).

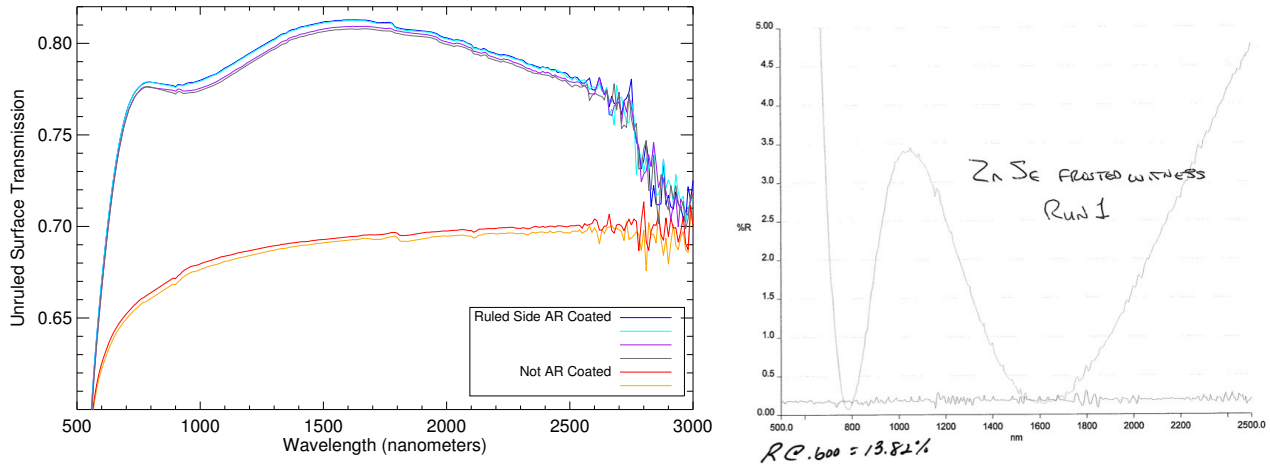

Figure 2. Transmission of the *unruled* area before/after coating a single surface. (Left) Total sample throughput before (red) and after (blue) AR coating. (Right) Measured reflectivity of the AR-coated surface of a frosted (on one side) witness sample.

4. BLAZE FUNCTION BEFORE / AFTER COATING

The ultimate check of a grism is its ability to produce a spectrum. This is why we measured the blaze function of the ruling sample, before and after the AR coating was applied. It is presented in Figure 3. The ruling sample was placed in a collimated beam immediately behind an aperture mask 5 mm in diameter to constrain light on the ruled surface. The beam was directly incident (perpendicular) to the surface. Lasers at 5 discrete wavelengths were used (632 nm, 904 nm, 1064 nm, 1310 nm and 1550 nm) to measure the flux both with and without the ruling sample in the beam. The ratio of the fluxes yielded the data points shown in Figure 3. To ensure flux stability at the level of $\leq 3\%$, lasers were turned on and left to thermalize for approximately one hour before measurements were obtained. We used an Hawaii-1 Teledyne detector cooled to liquid nitrogen temperature in the TRIDENT cryostat (ref) and performed aperture photometry on dark-subtracted and flat-fielded images. Uncertainty on each transmission data point is of order 3-4%.

A model of the blaze function was produced using PC Grate, a software that calculates electromagnetic wave transmission from first principles using the one-dimensional groove profile and material properties as inputs. A total of 16 actual AFM groove scans of the ruling sample (as in Figure 4) were modelled with PC Grate and averaged to construct the mean model presented here.

The peaks of the blaze function in order 1 (order 2) went from 59% (54%) to 73% (63%) by AR coating the ruled side. That is an improvement of about 11-15% across the spectrum in both orders, similar to the gain measured for the *unruled* part of the ruling sample (see previous section). We conclude that AR coating the ruled side of the sample is as effective as coating the unruled side in improving transmission.

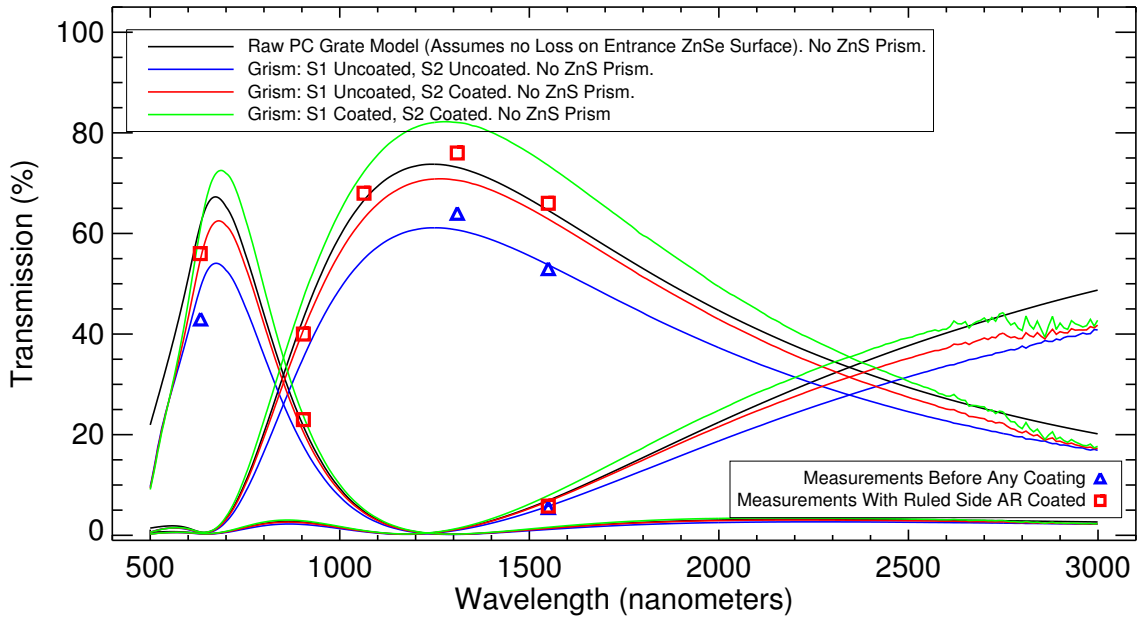

Figure 3. Effect on the blaze function of AR coating the ruled side of the Ruling Sample. The blue line and data are the modelled curve and lab measurements before any coating was applied. The red line and data are the same after the ruled side was AR coated. There is very good agreement between the model and the data. The uncertainty on the data points is about 1% but systematic errors are probably higher ($\leq 3-4\%$). The model is based on the PC Grate model scaled with the substrate and coating transmission measurements. The ZnSe grism with the ZnS prism are the two optics elements entering into the GR700XD device. This blaze function is for the ZnSe grism alone, not considering the ZnS prism.

5. GROOVE PROFILE BEFORE / AFTER COATING

Atomic force microscope (AFM) scans were obtained on the sample before and after AR coating (Figure 4). AFM images were acquired in air at room temperature using the tapping mode of a Digital Instruments Dimension 5000 microscope. Scans were obtaineds in five adjacent regions within a ≤ 1 mm^2 area with an offset of about 8 mm (along the grooves) and 3 mm (across the grooves) from the geometric center of the sample. Both AFM runs were done in the same area although the exact region could not be recovered. Typically, scans of regions 100×20 microns encompassing 4 to 5 grooves were followed by scans of 30×8 microns on a single groove. Table 1 gives the average depth and small facet width measured over all available scanned regions before and after coating. Within uncertainties, the groove geometry is unchanged.

Table 1. AFM Measured groove period and depth on the LLNL ruling sample before and after an AR coating was applied

	Period (μm)	N data	Depth (nm)	N data	Small Facet Width (nm)	N data
Pre Coating	18.51 ± 0.03	5	756 ± 15	26	0.72 ± 0.12	8
Post Coating	18.43 ± 0.05	9	772 ± 22	32	0.84 ± 0.09	15

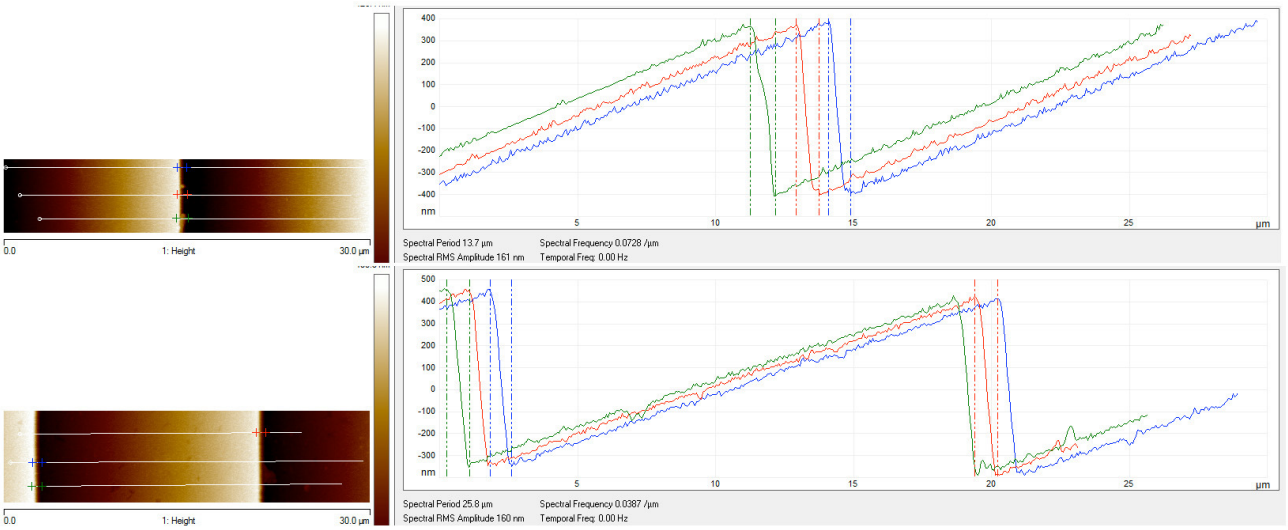

Figure 4. Atomic Force Microscopy of the ruling sample before (top) and after (bottom) an AR coating was applied on the grating. The scans are of representative grooves, not identically the same groove. It is remarkable that the groove shape is unaltered despite applying an AR coating that represents 35% of the groove depth.

6. WAVEFRONT ERROR BEFORE / AFTER COATING

A third line of evidence comes from obtaining wavefront error measurements of the surface. Maps of the surface were obtained in reflection using Zygo interferometers in LLNL (prior to coating) and in UdeM (after coating), see Figure 5. In Montreal, it was checked that maps using the different orders of reflection yielded the same results. Thw wavefront did not appear to degrade due to the AR coating. It shows very little WFE change from 0.219 to 0.161 waves (PtV) or 0.028 to 0.026 waves (RMS). This indicates that the coating did not alter the surface.

7. CRYOGENIC CYCLING

The Ruling Sample underwent a series of 3 cryogenic cycles to investigate the resistance of the AR coating. Each cycle used a cooling rate of 0.2 K/minute to bring the sample to a temperature of 16 K which was maintained for 24 h, after which the sample was warmed to room temperature at a rate of 0.2 K/minute. Three

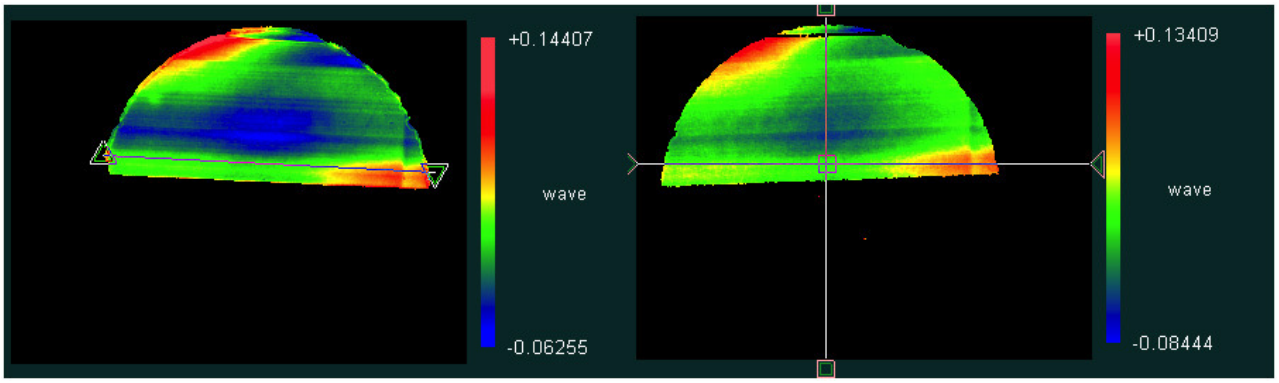

Figure 5. Wavefront error map of the ruled side of the ruling sample, before (left) and after(right) AR coating the sample. No change is noticed in the surface figure.

such cycles were performed without breaking the vacuum. The Kermit cryostat at UdeM was used with the sample directly attached on the cold bench with an aluminum cell. Microscope images of the ruled area were obtained immediately prior and after the cryogenic life test. Images were obtained at 35X using a Leica EZ4 HD microscope. Figure 6 shows a comparison of before/after photographs of the Ruling Sample at a position on the sample where tiny ($\leq 100\mu$m) bits appeared after cryo cycling. They ressemble particles created when scratching the surface with a blade. They occured sparsely accross the surface and were not dislodged by blowing dry air on them so pose minimum risk of contamination.

Figure 6. Pre (left) and post (right) cryogenic life test photographs at 35X magnification. Two purple objects appear post cryo. Their size is approximately 70 microns in diameter. After blowing dry air and revisiting the area, the objects remained there. They most probably are tiny substrate chips dislodged during cryo cycling. Their color to the naked eye is white. A few dozens were counted across the surface.

8. PROTON IRRADIATION

To simulate exposure to space radiations, we used a different sample, this time an AR coating sample deposited on a ZnS substrate. The AR coating was of the same design as that used for the ZnSe grism.

Depositing 6-year and 11-year equivalent of radiation exposures using 1 or 10 MeV protons requires calculating the efficiency of the sample material at absorbing the proton energy. If **c** is the proton cross section of the material (in eV $\times$ cm^2), **N** is the number of atoms per unit volume and **dE/dX** is the energy loss by a proton travelling

a distance **dX**, then:

$$\mathbf{c} = -1/\mathbf{N} \times \mathbf{dE}/\mathbf{dX} \tag{1}$$

or the energy loss for a given material thickness, dX, is:

$$\mathbf{dE} = -\mathbf{N} \times \mathbf{c} \times \mathbf{dX} \tag{2}$$

Deposited dose calculations for thin layers is much more uncertain than for thick substrates because the exact nature and thicknesses of AR coatings are not known but charge deposition is directly dependent on those parameters. Depending on the assumptions, implanted doses can vary by one or two orders of magnitudes. Also, in order to be effective at depositing charges in the AR coatings, we resorted on using lower energy protons (1 MeV rather than 10 MeV) simply because high energy particles tend to deposit very little of their energy on short scales.

At the time of irradiation the coating thickness was proprietary so its nature and thickness were unknown. We thus assumed a range of plausible cross sections (30 to 60 $\times 10^{-15}$ eV$\times$cm^2), number densities (.01 to 0.10 mol/cm^3) and thicknesses (100 to 1000 nm). The energy drop of the 1 MeV protons thus varies by two orders of magnitude in the range:

$$\begin{aligned} \mathbf{dE} = [0.01 - 0.10]\text{mol/cm}^3 &\times 6.022 \times 10^{23}\text{mol}^{-1} \\ &\times [30 - 60] \times 10^{-15}\text{eV} \times \text{cm2} \\ &\times [100 - 1000] \times 10^{-7}\text{cm} \\ &= [1.8 - 361]\text{keV} \end{aligned} \tag{3}$$

In other words, between 0.18% and 36.1% of a 1 MeV proton energy is absorbed by the coating. Expected life doses are generally specified for thick aluminum thicknesses. So, that means a scale factor between ~ 3 and ~ 500 was required to simulate what a thick sample would be exposed to (thick samples absorb all of the proton's energy).

We used the particle accelerator at Université de Montréal. It is a 6 mega Volt Tandem that can accelerate protons up to 10 MeV. Cumulative doses between 5×10^{11}, 1×10^{13} and 5×10^{14} protons/cm^2 were aimed at the ZnS AR-coated sample. One area had the coating directly facing the beam while the other area had the substrate facing the beam. We measured the transmission of the sample as a function of wavelength, after each irradiation (Figure 7). No transmission change was noticed after even the largest irradiation proving the toughness of the TFL coating.

9. CONCLUSIONS

Various tests and measurements were performed on the LLNL Ruling Sample before and after the ruled area was anti-reflection coated to investigate for any change induced by the coating. Measurements of the groove shape with an atomic force microscope showed no significant change in the shape, depth or separation of the grooves with 5 mesasurements on the sample. The Blaze Function was measured at 4 different wavelengths (632, 904, 1064, 1550 nm) in orders 0, 1 and 2. The curves before and after were both very consistent with our model transmission and expected gain from the coating transmission measurements on the bare sample. The wavefront error was measured using a Zygo interferometer after the sample was coated and showed a similar figure to that of the ruled surfaces of the 2 LLNL grisms with peak-to-valley errors around 0.1 wave over a cm2. Microscope inspection after a series of 3 cold life tests to 16 K for 24 hours showed a number (probably much less than 1%) of very small defects ($\leq$ 75 microns) appearing. They look like new pits on the surface rather than large flakes so are probably not delamination events. It is not clear if those defects are associated with the AR coating or if they would have occured on a naked ruled surface. We also verified that the WFE map of the large ruled area in reflection did not change after cryo cycling the sample. Our conclusions are that AR coating the ruled surface of the LLNL grism poses no measurable risk and improves the grism transmission by an amount of 10-14%, depending on wavelength.

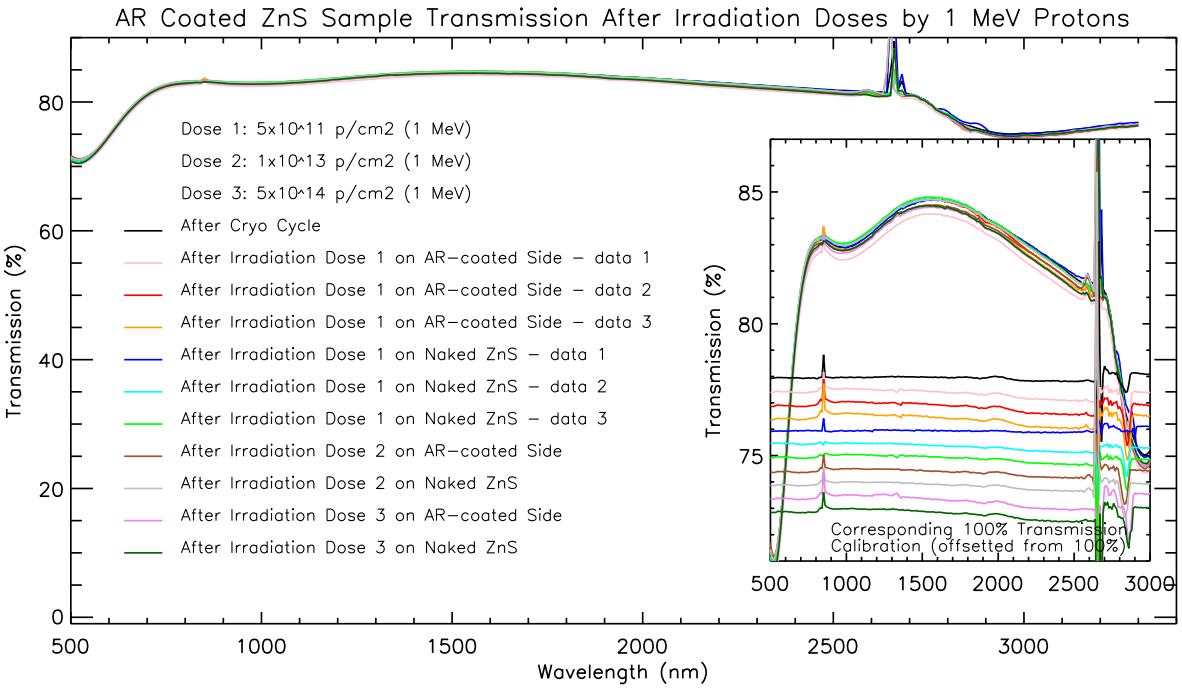

Figure 7. Transmission curve of an AR coating sample before and after a series of irradiation doses to 1 MeV protons. No change is noticed for cumulative doses between $5{\times}10^{11}$, 1×10^{13} and 5×10^{14} protons/cm^2.

ACKNOWLEDGMENTS

This work is financially supported by the Canadian Space Agency (contract #9F052-130055/001/MTB), the National Research Council of Canada, the National Science and Engineering Research Council of Canada, the Fond Québécois de Recherche - Nature et Technologie, and the Université de Montréal. Lawrence Livermore National Laboratory is operated by Lawrence Livermore National Security, LLC, for the U.S. Department of Energy, National Nuclear Security Administration under Contract DE-AC52-07NA27344.

REFERENCES

[1] Doyon, R., Hutchings, J. B., Beaulieu, M., Albert, L., Lafrenière, D., Willott, C., Touahri, D., Rowlands, N., Maszkiewicz, M., Fullerton, A. W., Volk, K., Martel, A. R., Chayer, P., Sivaramakrishnan, A., Abraham, R., Ferrarese, L., Jayawardhana, R., Johnstone, D., Meyer, M., Pipher, J. L., and Sawicki, M., "The JWST Fine Guidance Sensor (FGS) and Near-Infrared Imager and Slitless Spectrograph (NIRISS)," in [*Society of Photo-Optical Instrumentation Engineers (SPIE) Conference Series*], *Society of Photo-Optical Instrumentation Engineers (SPIE) Conference Series* **8442** (Sept. 2012).

[2] Kuzmenko, P. J., Little, S. L., Albert, L., Aldridge, D. A., Doyon, R., Maszkiewicz, M., and Touahri, D., "Diamond machining of ZnSe grisms for the Near Infrared Imager and Slitless Spectrograph (NIRISS) onboard JWST," in [*Society of Photo-Optical Instrumentation Engineers (SPIE) Conference Series*], *Society of Photo-Optical Instrumentation Engineers (SPIE) Conference Series* **9151** (June 2014).

[3] Skrutskie, M. F., Jones, T., Hinz, P., Garnavich, P., Wilson, J., Nelson, M., Solheid, E., Durney, O., Hoffmann, W., Vaitheeswaran, V., McMahon, T., Leisenring, J., and Wong, A., "The Large Binocular Telescope mid-infrared camera (LMIRcam): final design and status," in [*Society of Photo-Optical Instrumentation Engineers (SPIE) Conference Series*], *Society of Photo-Optical Instrumentation Engineers (SPIE) Conference Series* **7735** (July 2010).

[4] Kuzmenko, P. J., Little, S. L., Little, L. M., Wilson, J. C., Skrutskie, M. F., Hinz, P. M., Leisenring, J. M., and Durney, O., "Fabrication and testing of germanium grisms for LMIRcam," in [*Society of Photo-Optical*

Instrumentation Engineers (SPIE) Conference Series], *Society of Photo-Optical Instrumentation Engineers (SPIE) Conference Series* **8450** (Sept. 2012).

[5] Gully-Santiago, M., Wang, W., Deen, C., Kelly, D., Greene, T. P., Bacon, J., and Jaffe, D. T., "High-performance silicon grisms for 1.2-8.0 μm: detailed results from the JWST-NIRCam devices," in [*Society of Photo-Optical Instrumentation Engineers (SPIE) Conference Series*], *Society of Photo-Optical Instrumentation Engineers (SPIE) Conference Series* **7739** (July 2010).